

# Scattering induced dynamical entanglement and the quantum-classical correspondence

M. Lombardi and A. Matzkin

*Laboratoire de Spectrométrie physique (CNRS Unité 5588),*

*Université Joseph-Fourier Grenoble-1,*

*BP 87, 38402 Saint-Martin, France*

## Abstract

The generation of entanglement produced by a local potential interaction in a bipartite system is investigated. The degree of entanglement is contrasted with the underlying classical dynamics for a Rydberg molecule (a charged particle colliding on a kicked top). Entanglement is seen to depend on the structure of classical phase-space rather than on the global dynamical regime. As a consequence regular classical dynamics can in certain circumstances be associated with higher entanglement generation than chaotic dynamics. In addition quantum effects also come into play: for example partial revivals, which are expected to persist in the semiclassical limit, affect the long time behavior of the reduced linear entropy. These results suggest that entanglement may not be a pertinent universal signature of chaos.

PACS numbers: 03.65.Ud,05.45.Mt,34.60.+z,03.67.Mn

Entanglement, i.e. the nonseparability intrinsic to composite systems, is one of the most peculiar features of the quantum world. In its most popular form, found for example in the original EPR proposal [1], the entanglement is of geometrical nature. However any usual potential interaction between two particles can generically lead to entanglement, provided several quantum states are accessible to both particles. The study of such dynamical entanglement is particularly interesting for systems which possess a classical counterpart. Recent investigations have been focusing on the relation between the generation of entanglement and the underlying classical dynamics. Initial work in spin-boson systems [2] and in coupled kicked tops [3] suggested that chaotic dynamics generate more and faster entanglement, but this claim was subsequently revised [4, 5], in part due to discrepancies regarding the derivation of the classical limit [6]. Concurrently efforts are being made to derive universal relations ruling the generic generation of entanglement, irrespective of system specifics [7, 8, 9], but the predicted results differ according to the method employed and the approximations made. Thus, contrarily to the well established quantum-classical correspondence for spectral statistics and large scale fluctuations [10], an analog correspondence and the existence of universal regimes regarding the generation of entanglement is still debated and has recently been questioned [11, 12].

In this work we study the generation of entanglement for a real system which possesses an unambiguous classical counterpart. This will be done by employing a bipartite system where entanglement is produced by a *local* interaction, viz. the particles interact via a short-range scattering potential. We will see that the underlying classical dynamics is reflected in the generation of entanglement. However this dependence involves particular features in the structure of phase-space rather than the global dynamical (chaotic or regular) regimes. Quantum effects also come into play, particularly at long times.

The system investigated here is a Rydberg molecule. Simply stated, a Rydberg molecule is composed of two parts: a highly excited electron on the one hand, and a compact ionic molecular core, containing the nuclei and the tightly bound other electrons on the other. Most of the time, the outer electron and the core are spatially well-separated: the core rotates freely with angular momentum  $\mathbf{N}$  and energy  $E_N^+ \propto N^2$ , whereas the outer electron senses a pure Coulomb field. Its orbital angular momentum  $\mathbf{L}$  is fixed in space. Seen in the molecular frame  $\mathbf{L}$  turns around the  $\mathbf{N}$  axis (with polar angles  $\theta$  and  $\varphi$ , see Fig. 1(a)). However, the outer electron periodically scatters on the molecular core. Classically

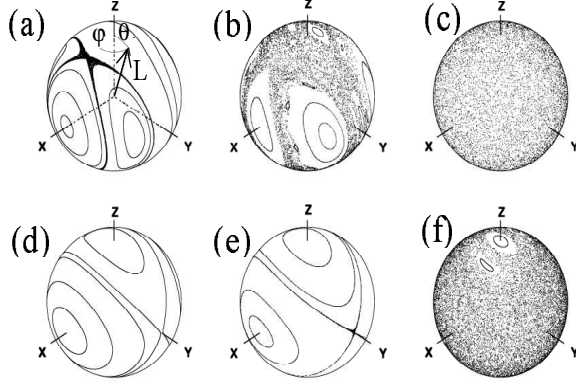


FIG. 1: Poincaré surfaces of section in the molecular frame. The core axis is along  $OZ$  and  $\mathbf{N}$  along  $OX$ . Top row: generic case, (a):  $k = 0.25$ , (b):  $k = 0.5$ , (c):  $k = 10$ . Bottom row: same values of  $k$  for the resonant case  $T_e = T_0$ . (a) also shows the angles  $\theta$  and  $\varphi$  for a given position of  $\mathbf{L}$  on the sphere.

the electron is kicked by the rotating core. This kick results in a change in the direction of  $\mathbf{L}$  by  $\Delta\varphi$ , the deflection angle of the plane of the classical Kepler orbit.  $\mathbf{N}$  adjusts accordingly, since the total angular momentum  $\mathbf{J} = \mathbf{L} + \mathbf{N}$  is conserved. The conservation of  $\mathbf{L}$  and the cylindrical symmetry of the core implies that  $\Delta\varphi = k \cos\theta$  where  $k$  gives the strength of the kick. A negligibly small kick yields regular dynamics. This is visualized in a Poincaré surface of section obtained by plotting the position of  $\mathbf{L}$  after each kick (Fig. 1) [13]. For very small  $k$ ,  $\mathbf{L}$  encircles the  $\mathbf{N}$  axis, meaning that  $\mathbf{L}$  is fixed in space, and thus that on a given circle, the modulus  $N$  is constant. As  $k$  increases, two cases must be distinguished. In the generic case [Figs. 1(a)-(c)], a chaotic sea progressively takes over until the last islands of regularity disappear. Things are different in the resonant case. Resonances appear when the orbital period of the electron  $T_e$  and the rotational period of the core  $T_0$  are commensurate, so resonances are nongeneric. At resonances, chaos is inhibited and only appears along the separatrix [Figs. 1(c)-(f)]. The chaotic sea takes over for values of  $k$  larger than in the generic case. Resonances are known to modify the spectrum of small Rydberg molecules, such as the stroboscopic effect experimentally observed on  $\text{Na}_2$  [14].

In quantum-mechanical terms the collision couples the electron and core dynamics and induces phase-shifts in the wavefunction of the outer electron. In the absence of the core-electron interaction, the Hamiltonian  $H_0$  is separable and the eigenstates are given by the

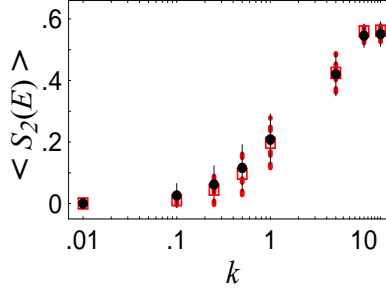


FIG. 2: Average linear entropy for generic (red/gray boxes) and resonant (black dots) states ( $T_e = T_0$ ), shown for different values of  $k$ . The rms is also shown as red dashed (generic) and solid (resonant) error bars.

product state

$$\phi_N(E, r) = f_L(E - E_N^+, r) \otimes |N\rangle \quad (1)$$

where  $E$  is the total energy,  $|N\rangle$  the state of the core and  $f_L$  the radial Coulomb function of the electron whose energy is  $\epsilon_N = E - E_N^+$  [15]. The total Hamiltonian  $H = H_0 + V$  includes the core-electron interaction potential  $V$ . The eigenstates are given from scattering theory by

$$\psi(E, r) = \sum_N Z_N(E) [I + G_0(E)K] \phi_N(E, r), \quad (2)$$

where  $G_0$  is the Green's function,  $Z_N$  are expansion coefficients and  $K$  is the scattering matrix, whose elements  $K_{N'N}$  are related to the transition probability amplitude between states  $\phi_N$  and  $\phi_{N'}$  due to the collision. From Eq. (2) it is apparent that an eigenstate is given by a superposition of core states with rotational number  $N$ , each core state being associated with an outer electron having an energy  $\epsilon_N$ . The relation between the quantum and classical pictures is simpler [13] when expressed in the molecular frame, where  $K$  has only diagonal elements  $\tan \delta_\Lambda$ . The phase-shifts  $\delta_\Lambda$  only depend on the coupling between  $\mathbf{L}$  and the molecular axis.  $\Lambda = L \cos \theta$  is the projection of  $\mathbf{L}$  on this axis and the classical deflection angle is related to the quantum phase shifts by

$$\Delta\varphi = 2 \frac{\partial \delta_\Lambda}{\partial \Lambda} = k \frac{\Lambda}{L}. \quad (3)$$

The first equality is a very general result stemming from the semiclassical approximation to scattering theory [16] and is valid to first order in  $\hbar$ , whereas the last term follows from the functional relation  $\delta_\Lambda(k)$  chosen in this work which turns out to be verified for typical diatomic molecules.

To quantify entanglement we will compute the linear entropy  $S_2$  associated with the reduced density matrix describing the electron

$$S_2 = 1 - \text{Tr}_e \rho_e^2, \quad (4)$$

where  $\rho_e = \text{Tr}_c \rho$  and as usual  $\text{Tr}_c$  ( $\text{Tr}_e$ ) refers to averaging over the core (electron) degrees of freedom. We first determine the degree of entanglement of stationary states. This is done by calculating  $\rho(E) = |\psi(E)\rangle \langle \psi(E)|$  over an energy range for which the classical dynamics does not vary appreciably. The values  $L = 2$  and  $J = 10$  adopted in this work correspond to experimentally accessible values for diatomic molecules such as  $\text{Na}_2$ . With these values and taking into account symmetry requirements, three rotational states are accessible to the core  $N = 8, 10, 12$  (classically,  $8 \leq N \leq 12$ ). Hence in a typical eigenstate (2) three core-electron states are entangled. The mean entropy  $\langle S_2(E) \rangle$  for stationary states is shown in Fig. 2 as a function of the coupling constant  $k$ . The curves for the generic and resonant cases are very close despite phase-space being substantially different for most values of  $k$ . On average the potential interaction entangles at least as efficiently when the underlying classical dynamics is mostly regular rather than mainly chaotic. Note the rms is small for the regular and totally chaotic regimes and larger in the mixed phase-space situation and that the linear entropy saturates in both the generic and resonant cases only for large  $k$ :  $\langle S_2(E) \rangle$  approaches its upper limit  $2/3$  corresponding to a maximally mixed state.

We next determine the time-dependent generation of entanglement from an initial product state. At  $t = 0$  we take the wavefunction of the electron to be radially localized at the outer turning point  $r_{tp}$ , several thousand atomic units away from the core, and we take the core to be in the rotational state  $|N_0\rangle$ , so that

$$\psi(t = 0, r) = F_{loc}(r \approx r_{tp}) \otimes |N_0\rangle. \quad (5)$$

The mean energy of the radial wavepacket  $F_{loc}$  is  $\epsilon_0 = E_0 - E_{N_0}^+$  and  $T_e$  is the period of the corresponding Kepler orbit. At  $t \approx T_e/2$  the wavepacket scatters off the core and the wavefunction is given by a *superposition* of radial wavepackets moving outward, each associated with a core in a given rotational state  $|N\rangle$ . At  $t \approx T_e$  each of the radial wavepackets has reached the outer turning point and starts going back towards the core. The core-electron interaction then takes place again at  $t \approx 3T_e/2$  resulting in further entanglement change. As  $t$  increases the wavepackets tend to spread radially resulting in a continuous core-electron

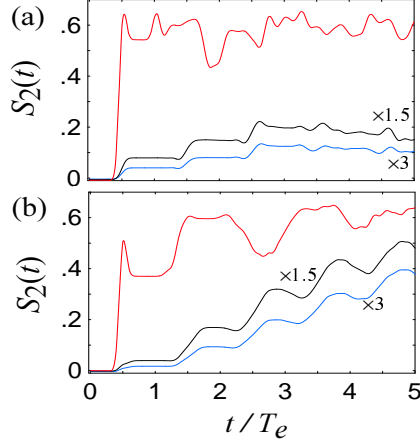


FIG. 3: Short time variation of the linear entropy for different values of the coupling strength;  $t$  is given in units of the Kepler period  $T_e$ . (a) Generic phase-space, from top to bottom  $k = 10$  (red), 0.5 (black) and 0.25 (blue). The  $k = 0.25$  ( $k = 0.5$ ) curve is multiplied by a factor 3 (1.5). (b) Same as (a) for the resonant case  $T_e = T_0$ .

interaction. These features appear in the time dependence of the linear entropy  $S_2(t)$ , obtained from Eq. (4) by tracing out the core degrees of freedom from the total density matrix  $|\psi(t)\rangle\langle\psi(t)|$ .

For short times  $S_2(t)$  is shown in Fig. 3, for  $N_0 = 8$  and for 3 different values of the coupling  $k$ . In the generic case, for small  $t$  and not too large  $k$ ,  $S_2$  is seen to increase linearly in steps, reflecting the discrete times core-electron interaction, and then appears to saturate (but see below). In the resonant case, the linear entropy also increases on average linearly but displays oscillations. Indeed, a semiclassical approximation for the short-time behavior of the purity  $\text{Tr}_e \rho_e^2$  predicts that  $S_2(t_C) \propto k^2 t_C$ . This result, valid only for the collision times  $t_C = (2m + 1)T_e/2$ , is obtained in the stationary phase approximation by neglecting correlations between electron orbits built on different core rotational states. This linear behavior agrees with the prediction of [9]. The  $k^2$  dependence comes from the semiclassical amplitudes, and the linear variation in  $t$  from the fact that these amplitudes are conserved.

The oscillations of  $S_2$  observed in the resonant case arise from the coherent projection of the motion of the outer electron. It is in this sense a kinematical effect, since no such behavior is to be found in the wavefunction or in the probability flux. By expanding the

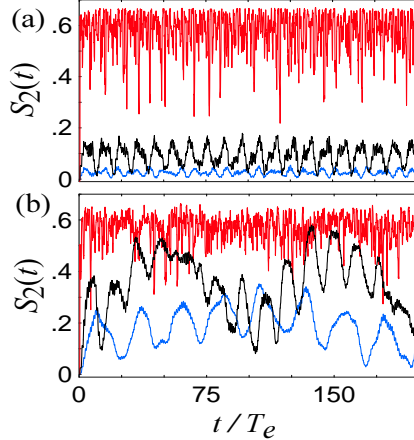


FIG. 4: Same as Fig. 3 for longer times; the curves for  $k = 0.25$  and  $k = 0.5$  are *not* multiplied by any factor. The oscillations visible for these curves depend on the revival time of the partial correlation functions. For example in (b) for  $k = 0.5$ , two scales are visible corresponding to  $T_e^{rev}(N = 10)$  and the longer  $T_e^{rev}(N = 12)$ .

core energies to first order, the purity is seen to depend on terms of the form

$$\sum_{NN'} e^{2i\pi t[(N-N')/T_0]} \sum_{\epsilon(N)\epsilon'(N')} e^{-i(\epsilon-\epsilon')t} Z_N(E) Z_{N'}(E') \langle F_L(\epsilon'(N')) | F_L(\epsilon(N)) \rangle, \quad (6)$$

where  $\epsilon_N = E - E_N^+$  and  $F_L(\epsilon, r)$  are radial functions on the energy shell (i.e. a combination of regular and irregular Coulomb functions with effective phase shifts depending on the scattering matrix  $K$ ). These functions form an overcomplete basis and are not orthogonal in  $\epsilon$ . In the generic case the nondiagonal terms in the second sum are generally small and uncorrelated. However at resonance both exponentials are in phase (since  $\epsilon - \epsilon' \approx 2m\pi/T_0$ ) and the correlations between nondiagonal terms are enhanced, because the resonance imposes a greater similarity of the eigenstates (2) [13].

The long time behavior of the entanglement production is shown in Fig. 4. In the generic case,  $S_2(t)$  is on average very low for  $k = 0.25$  (corresponding to classically regular phase space), higher for  $k = 0.5$  (mixed phase-space) and nearly maximal for  $k = 10$  (chaotic phase space). Periodic recoherences are visible for small  $k$ . Although revivals are expected when phase space is regular and the dimensionality of the Hilbert space is low, we point out that the same observations have been made for considerably larger angular momenta closer to the semiclassical limit [17]. The characteristic periods of recoherence involve the revival times  $T_0^{rev}$  and  $T_e^{rev}$  of the core rotation and the electron orbit. The former readily

appears by carrying the expansion in  $E_N^+$  in Eq. (6) to second order. The latter follows by remarking that the second sum in Eq. (6) is the cross-correlation function between parts of the wavefunction belonging to different superposition alternatives (i.e. different scattering channels). Alternatively, it can be shown [18] that the purity is bounded from below by correlation functions which vary according to the revival times. Note that the revivals have no classical counterpart (they are much shorter than the Poincaré recurrence time). In the resonant case the long-range oscillations can be dramatically enhanced by the commensurate time scales (in addition to  $T_0 = T_e$ , we have  $T_0^{rev} \approx 2T_e^{rev}$ ) and the similarity of the eigenfunctions which makes the cross-correlations to be very large. The consequence is that the curves for  $k$  values corresponding to different underlying classical dynamics may cross.

These results indicate that the behavior of the linear entropy is not simply connected to the classical regime, but also depends on the structure of phase-space. Indeed the entanglement production is considerably *higher* in the resonant case despite classical phase space being much more *regular* (compare Figs. 1(b) and (d) with their respective curves in Fig. 4). Note also that in the generic case the time average of  $S_2(t)$  reflects the average entanglement of the stationary states shown in Fig. 2; but this is not so at resonance, where the time average of  $S_2(t)$  is considerably higher. This behavior can be ascribed to the large values of the cross correlations, which are ultimately due to the fact that at resonance  $\mathbf{L}$  appears to move with the core, and therefore its projection on  $\mathbf{N}$  (and thus the possible values of  $N^2$ ) tend to spread. Classically, resonances modify the structure of phase-space by the appearance of a fixed point on the  $OZ$  core axis, which is visible in the Poincaré surfaces of section (Fig. 1). In quantum mechanical terms  $N$  is then not well-defined and thus the wavefunctions are mixed in  $|N\rangle$  even for small kick strengths. In the generic case however these mixings can only take place for large values of the coupling, corresponding to chaotic dynamics.

To conclude we have investigated the generation of entanglement induced by a potential interaction in a bipartite system, a Rydberg molecule. By and large chaotic classical dynamics is associated with more and faster entanglement because the scattering particles explore larger portions of phase-space leading quantum-mechanically to superpositions. But chaos is not necessarily the most efficient way to ensure that the relevant part of phase-space leading to superpositions (in our system the rate of inelastic scattering) is explored

with a large classical amplitude: this is why a dynamical effect such as resonances generate higher entanglements despite classical phase-space being mostly regular. The present observations support similar results obtained from random matrix models or for coupled kicked tops [6, 11, 12]. We have also seen the existence of specific nonclassical effects in the time evolution of the linear entropy, such as the kinematical short time oscillations observed for resonant states and the dynamical oscillations arising from partial wavepacket revivals for long times. Similar long time recoherences were recently observed in a model describing coupled Bose-Einstein condensates [8].

We are grateful to T. H. Seligman (UNAM, Cuernavaca, Mexico) for fruitful discussions.

- 
- [1] A. Einstein, B. Podolsky and N. Rosen, Phys. Rev. 47, 777 (1935).
  - [2] K. Furuya, M. C. Nemes and G. Q. Pellegrino, Phys. Rev. Lett. 80, 5524 (1998).
  - [3] P. A. Miller and S. Sarkar Phys. Rev. E 60, 1542 (1999).
  - [4] H. Fujisaki, T. Miyadera, and A. Tanaka Phys. Rev. E 67, 066201 (2003)
  - [5] M. Novaes and M. A. M. de Aguiar, Phys. Rev. E 70, 045201(R) (2004).
  - [6] J. N. Bandyopadhyay and A. Lakshminarayan Phys. Rev. E 69, 016201 (2004)
  - [7] Ph. Jacquod, Phys. Rev. Lett. 92, 150403 (2004)
  - [8] R. M. Angelo and K. Furuya, Phys. Rev. A 71, 042321 (2005).
  - [9] M. Znidaric and T. Prosen Phys. Rev. A 71, 032103 (2005)
  - [10] F. Haake, *Quantum signatures of chaos* (Springer, Berlin, 2001).
  - [11] T. Gorin and T.H. Seligman, Phys. Lett A 309 61 (2003).
  - [12] R. Demkowicz-Dobrzanski and M. Kus Phys. Rev. E 70, 066216 (2004)
  - [13] B. Dietz, M. Lombardi and T. H. Seligman, Ann. Phys. 312, 441 (2004). M. Lombardi et al., J. Chem. Phys. 89, 3479 (1988).
  - [14] P. Labastie et al., Phys. Rev. Lett. 52, 1681 (1984); E. S. Chang et al. J. Chem. Phys. 111, 6247 (1999).
  - [15] The angular part of the electron wavefunction is contained in the compound notation  $|N\rangle$  due to the coupling of angular momenta. This 'geometrical entanglement' plays no role in this work which focuses on the superpositions in  $\mathbf{N}^2$  and not in the relative orientations of the angular momenta.

- [16] R. G. Newton, *Scattering theory of waves and particles* (Springer, New-York, 1982), Ch. 18.
- [17] M. Lombardi and A. Matzkin, in preparation.
- [18] T. Prosen, T. H. Seligman and M. Znidaric, Phys. Rev. A 67, 062108 (2003).